Basic Neuroscience

Longitudinal assessment of infarct progression, brain metabolism and behavior following anterior cerebral artery occlusion in rats

Heike Endepols[*], Hanna Mertgens, Heiko Backes, Uwe Himmelreich[2], Bernd Neumaier[1], Rudolf Graf, Günter Mies

Max Planck Institute for Neurological Research, Gleueler Str. 50, 50931 Koeln, Germany

HIGHLIGHTS

- We established an endothelin-1 model of anterior cerebral artery occlusion (ACAo).
- Autoradiography and PET disclosed transient gradual ischemia of up to 4 h.
- Comparable to abulia in humans, goal-directed executive functions deteriorated.
- In contrast, hyperactivity predominated, if task-related stimuli were absent.
- The model is well suited to study functional impairment and recovery after ACAo.

ARTICLE INFO

ABSTRACT

Background: Stroke patients suffering from occlusion of the anterior cerebral artery (ACAo) develop cognitive and executive deficits. Experimental models to investigate such functional impairments and recovery are rare and not satisfyingly validated.

New method: We stereotactically injected the vasoconstrictor endothelin-1 (ET-1) close to the ACA of rats and assessed magnitude and course of CBF reduction using [^{14}C]iodoantipyrine autoradiography and [^{15}O]H$_2$O-PET. [^{18}F]FDG-PET and T2-weighted MRI determined regional metabolic and structural alterations. To test cognitive and executive functions, we analyzed decision-making in a food-carrying task, spatial working memory in a spontaneous alternation task and anxiety in an elevated plus maze test before and 1 month after ACAo.

Results: CBF decreased immediately after ET-1 injection, started to recover 1–2 h and returned to control 4 h thereafter. Metabolic and structural lesions developed permanently in the ACA territory. Hypometabolism occurring bilaterally in the piriform region may reflect diaschisis. Behavioral testing after ACAo revealed context-dependent changes in decision making, exploratory activity and walking speed, as well as decreased anxiety and spatial working memory.

Comparison with existing method(s): Aside from modeling a known entity of stroke patients, ACAo in rats allows to longitudinally study deterioration of cognitive and executive function without major interference by disturbed primary motor function. It complements therefore stroke research since common models using middle cerebral artery occlusion (MCAo) all affect motor function severely.

Conclusion: The established ACAo model in rats effectively reflects deficits characteristic for ACA stroke in humans. It is furthermore highly suitable for longitudinal assessment of cognitive and executive functions.

* Corresponding author. Present address: Institute of Radiochemistry and Experimental Molecular Imaging, University Hospital of Cologne, Kerpener Str. 62, 50937 Köln, Germany. Tel.: +49 0221 4726 227; fax: +49 0221 4726 298.
E-mail address: heike.endepols@uk-koeln.de (H. Endepols).
[1] Present address: Institute of Radiochemistry and Experimental Molecular Imaging, University Hospital of Cologne, Kerpener Str. 62, 50937 Koeln, Germany.
[2] Present address: Biomedical NMR Unit/MOSAIC, KU Leuven, O&N I Herestraat 49, Leuven 3000, Belgium.

1. Introduction

With almost 17 million strokes per year worldwide (Feigin et al., 2014), 1.3–3.0% ischemic strokes in the territory of the anterior cerebral artery (ACA) (Arboix et al., 2009; Bogousslavsky and Regli, 1990; Gacs et al., 1983; Kumral et al., 2002) lead to the considerable number of 220,000–507,000 new ACA patients annually. These patients may suffer from discrete motor dysfunction but the most prominent symptoms after ACA stroke are cognitive and executive impairments (Kumral et al., 2002; Kang and Kim, 2008; Nagaratnam et al., 1998). Thorough cognitive/executive testing has been confined to case studies (Bird et al., 2004), revealing decreased ability to perform voluntary actions (abulia) (Bogousslavsky, 1994). Abulia refers to the reduction of spontaneous speech and to Parkinson-like symptoms such as bradykinesia and hypokinesia (Kumral et al., 2002; Nagaratnam et al., 2004). More extensive cognitive analyses have been performed with patients suffering from a rupture of anterior communicating artery aneurysms, which results in ischemia analog to ACA strokes (Böttger et al., 1998; Hütter and Gilsbach, 1992; Martinaud et al., 2009). According to the mentioned studies, deficits in anterograde and retrograde memory, selective attention, task switching, planning, decision-making and concept formation are likely to occur.

Unlike experimental models of middle cerebral artery occlusion (MCAo), models of the occlusion of the anterior cerebral artery (ACAo) are only sporadically used. They may, however, serve as models not only for this specific entity of human stroke but also, in a more general sense, as models for the longitudinal study of cognitive and executive function after stroke. An advantage is that primary motor areas are supplied by the MCA, and therefore are not directly affected by ACAo. In consequence, it is possible to use behavioral tasks for the study of ischemia-induced cognitive changes without major interference by disturbed motor function. Previous behavioral experiments (simple and choice reaction time tasks) 2 and 3 weeks after ACAo suggested that motivation and attention remained intact, but executive functions were possibly impaired (Ward et al., 1998).

We first (study 1) developed and validated a rat model of ACA occlusion (ACAo) on the basis of earlier work (Ward et al., 1998) using the vasoconstrictor endothelin-1 (ET-1) to occlude the ACA. Our goal was to verify that ET-1 injection in proximity to the ACA results in a pronounced reduction of cerebral blood flow (CBF) for a time span long enough to produce ischemic damage (Hossmann, 1994). We investigated the magnitude of CBF reduction using quantitative [^{14}C]iodoantipyrine autoradiography, and the acute time course using repetitive [^{15}O]H$_2$O μPET.

The second goal (study 2) was to investigate executive functions longitudinally during the first month after ACAo. The main behavioral paradigm mimicked a natural foraging situation, where rats encounter food in the open and have to decide how to deal with it: either eat it at the food patch or carry it to their burrow (Takahashi and Lore, 1980). These food-handling decisions were studied in a meander maze where food was laid out, with the rat's home cage attached. Because spatial working memory and anxiety are important factors influencing decision-making in our food-carrying task, these functions were additionally investigated using a spontaneous alternation test in the Y-maze and an elevated plus maze test. Here we report ACAo-induced behavioral alterations and alterations of regional metabolic brain activity in affected brain areas.

2. Materials and methods

2.1. Animals

Experiments were carried out in accordance with the EU directive 2010/63/EU for animal experiments and the German Animal Welfare Act (TierSchG, 2006), and were approved by regional authorities (LANUV NRW). For validation of the ACAo model (study 1), 13 male Lister hooded rats (approx. 10 weeks old; Harlan, Borchen, Germany) were used to quantify CBF reduction with [^{14}C]iodoantipyrine autoradiography, and two for repetitive intraindividual CBF measurements using [^{15}O]H$_2$O μPET imaging. In the behavioral study (study 2), 26 rats (approx. 10 weeks old at start) were used for behavioral testing, and a subgroup of 10 rats underwent sequential PET imaging. All rats were pair-housed and maintained in an inverted 12-h light/dark cycle (lights on at 8 pm). While rats for autoradiography and repetitive CBF measurements were fed ad libitum, rats used for the behavioral study obtained a restricted diet of 80% of their free-feeding amount of food (2018 Teklad global 18% protein rodent diet; Harlan; 15–20 g) per day. Animals were weighed twice per week. Body weight was 276–324 g at the start of experiments.

2.2. Intracerebral ET-1 injection for ACA ischemia

ACAo or sham operation took place after the first sequence of behavioral testing and was performed by a single injection of ET-1 or vehicle near the pericallosal part of the ACA. Rats were anesthetized using 5% isoflurane (delivered in 70% N$_2$O and 30% O$_2$) and fixed in a stereotactic frame, where isoflurane concentration was reduced to 2.5%. Body temperature was measured with a rectal probe, and held constant at 37 °C using a heating pad. After removing skin and periost, a small hole (approx. 1 mm in diameter) was drilled midline 1.5 mm rostral from bregma, and the 26 G cannula of a Hamilton syringe was inserted 3 mm deep, measured from the level of the dura mater. ET-1 (150 pmol in 0.3 μl sterile PBS) was then injected with a rate of 0.2 μl/min in close proximity of the ACA (Fig. 1D). In sham operated animals, 0.3 μl PBS was injected. The cannula was left in place for 10 min, and then retracted. Minor bleeding from the sagittal sinus, which was pierced by the passage of the cannula, occurred in most cases. After the bleeding had stopped (after approx. 1 min), the burr hole was closed using bone wax and the skin wound was sutured followed by application of a local anesthetic (Lidocain gel).

2.3. Quantitative autoradiographic CBF measurements (study 1)

For autoradiography, 13 rats were initially anesthetized with 5% isoflurane in 70% N$_2$O and 30% O$_2$ and maintained at 2% isoflurane. Rectal temperature was kept at 37 °C using a feedback-controlled heating system. Polyethylene catheters were inserted into both femoral veins and arteries for i.v. tracer application and arterial sampling for blood gas analysis and tracer input function. Two time points were chosen: early ischemia (17–20 min; 5 ET-1 injected rats and 3 shams), and later ischemia (2 h; 3 ET-1 and 2 shams).

The [^{14}C]iodoantipyrine (IAP) technique was employed as described previously (Sakurada et al., 1978). Ten μCi/100 g body weight of [^{14}C]IAP dissolved in 1 ml of 0.9% saline (specific activity 55 mCi/mmol; Biotrend GmbH, Cologne, Germany) was applied via i.v. ramp infusion while taking arterial blood samples onto pre-weighed filter paper. After 60 s, animals were sacrificed by i.v. injection of saturated KCl solution to stop tracer delivery to the brain. Brains were removed quickly, frozen in methylbutane at −40 °C, and stored at −80 °C. Blood samples were weighed immediately after termination of experiments and placed in counting vials. A 5 ml scintillation cocktail was added, and [^{14}C]-radioactivity was measured in a scintillation counter (Wallace 1410, Pharmacia, Freiburg, Germany) using external quench correction.

Brains were cut into 20 μm cryostat sections (Leica CM3050, Leica Microsystems GmbH, Wetzlar, Germany), which were dried on a heating plate to prevent diffusion of the radioactive tracer. Sections were exposed to autoradiographic film (Hyperfilm ECL,
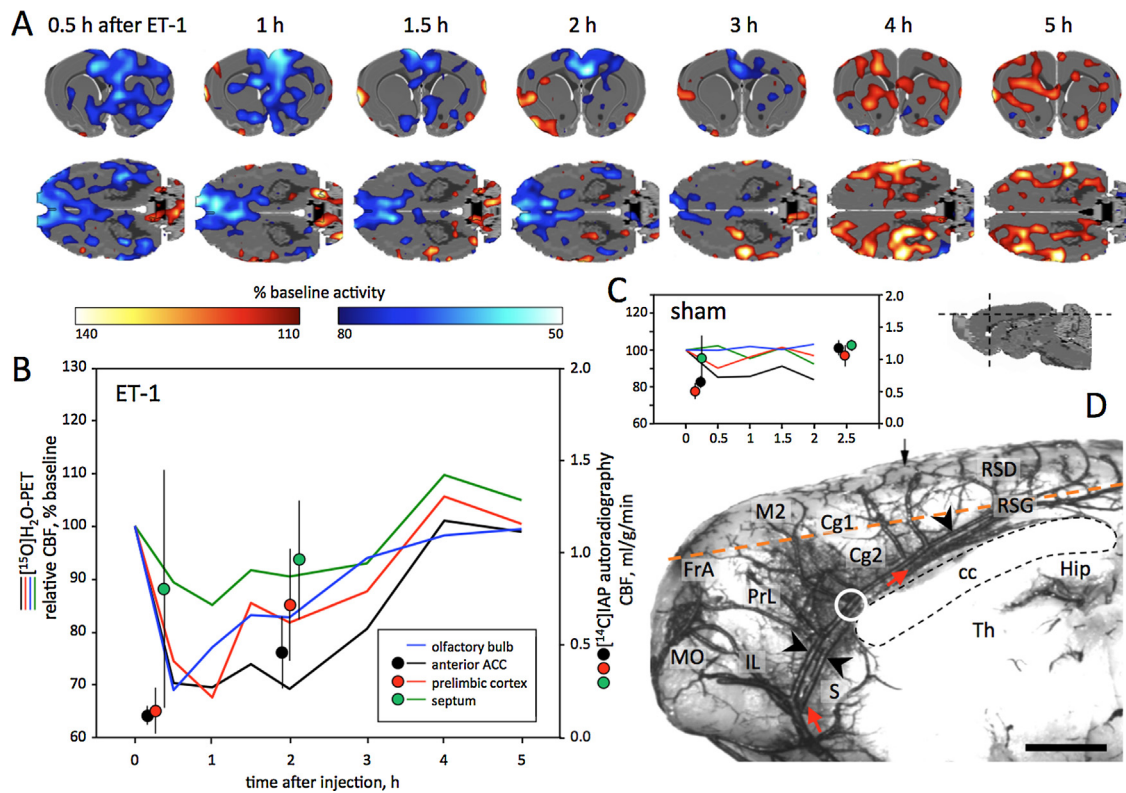
Fig. 1. CBF measurements after ACAo. (A) Regional changes of relative CBF (intensity normalized to cerebellum) at different time points (30 min–5 h) after ACAo, measured with $[^{15}O]H_2O$-PET in one animal. Shown is % change relative to baseline, i.e., before ACAo. Decrease (80–50% baseline) is indicated in blue, increase (110–140% baseline) in red. Dashed lines in the sagittal image below 5 h indicate level of horizontal (first row: 2.0 mm below bregma) and transverse sections (second row: 1.5 mm anterior to bregma). (B) Relative CBF values measured with $[^{15}O]H_2O$-PET (lines: left ordinate) from the same animal shown in (A). Superimposed are quantified CBF values measured with $[^{14}C]IAP$ autoradiography (filled circles; right ordinate; mean ± standard deviation) at two time points (17 min after ACAo, $n=5$; and 2 h after ACAo, $n=3$). The olfactory bulb was not analyzed with $[^{14}C]IAP$ autoradiography. (C) Relative and absolute CBF values similar to B with one sham animal for PET and five for autoradiography. (D) ET-1 injection site (white circle), shown in a medial view of the right telencephalic hemisphere (left hemisphere removed; anterior is left). Blood vessels are filled with latex and black ink. This rat had a double pericallosal ACA (black arrowheads), with both vessels giving off branches to the right and left medial cortices. Direction of blood flow is indicated by red arrows, bregma with a black arrow. The orange dashed line indicates the location of the profiles shown in Figs. 3 and 5. Abbreviations: cc: corpus callosum; Cg1 and 2: cingulate cortex 1 and 2; FrA: frontal association cortex; Hip: hippocampus; IL: infralimbic cortex; M2: secondary motor cortex; MO: medial orbital cortex; PrL: prelimbic cortex; RSD: retrosplenial dysgranular cortex; RSG: retrosplenial granular cortex; S: septum; Th: thalamus. Scale bar: 2 mm.

GE Healthcare Europe GmbH, Munich, Germany) with calibrated $[^{14}C]$-polymer standards for 12 days. After film development autoradiograms were digitized using a charge-coupled device camera (Sony SSCM370CE, Sony Incorporation of America, Cypress, CA, U.S.A.) operated by a Macintosh IIfx computer. Image processing was carried out with ImageMG, a user-revised version of the public domain program NIH-Image (W. Rasband, National Institutes of Health, Bethesda, MD, USA). Local CBF values from the autoradiograms were calculated with the in-build operational equations employing local tissue $[^{14}C]$-radioactivities and corresponding $[^{14}C]$-input functions. Due to the quick removal of the brain the olfactory bulb was damaged in most of the animals, so that this region was not analyzed with IAP autoradiography.

2.4. μPET imaging

PET scans were performed in a Focus 220 μPET scanner (CTI/Siemens Knoxville, TN; resolution at center of field of view: 1.4 mm) under isoflurane anesthesia. Respiratory rate was held at 50–70 breaths per minute by manually adjusting isoflurane concentration (2.0–2.5% delivered in 70% N_2O and 30% O_2). Body temperature was measured with a rectal probe and held at 37 °C using warm water flow through the animal holder. A transmission scan of approx. 10 min with a ^{68}Ge source was used for attenuation correction of all scans.

For the repetitive CBF protocol (study 1), two animals were used. $[^{15}O]H_2O$ (1.9–2.6 mCi in 500 μl) was injected via a tail vein in the baseline scans, and through a catheter in the femoral vein at later time points. One rat underwent ACAo and the other sham operation. CBF was measured every 30 min for 2 h, beginning approx. 30 min after ET-1/sham injection. In the ET-1 injected rat, CBF was subsequently measured every full hour up to 5 h after occlusion. After the end of PET scans, the rats were sacrificed by injecting 2 ml saturated KCl through the venous catheter.

In the behavioral study (study 2), 10 rats (8 ET-1, 2 shams) were measured. $[^{15}O]H_2O$ (1.0–1.8 mCi in 0.5 μl) was injected via a tail vein before and 40–61 min after ACAo. Emission data were acquired for 5 min, starting with tracer injection. After Fourier rebinning, data were reconstructed using two-dimensional filtered back projection, resulting in voxel sizes of 0.48 mm × 0.48 mm × 0.82 mm. In the same animals, $[^{18}F]$fluorodeoxyglucose (FDG; 0.9–1.5 mCi in 500 μl, injected through a tail vein) was used to investigate glucose metabolism. Emission data acquisition was 1 h starting with tracer injection. The rats underwent three metabolic scans: Before, 63–80 min, and 1 month after ACAo. Fourier rebinning was followed by an OSEM3D/MAP reconstruction (Qi et al., 1998), yielding voxel sizes of 0.38 mm × 0.38 mm × 0.82 mm.

Images were analyzed with the help of the imaging tool VINCI (Vollmar et al., 2007), where all images were manually co-registered. Intensity ratio normalization was performed using the

cerebellum as a reference region. Relative values are accordingly given as % cerebellum.

To demonstrate the ischemic lesion in the brain midline, a profile analysis was carried out over all images. A profile (length: 25.3 mm, width 2.0 mm) was placed on a horizontal section at a depth of 1.8 mm from dorsal brain surface (Fig. 1D, orange dashed line; Fig. 3B; Fig. 5B). Mean profile plots (data point spacing: 160 μm) were drawn for each time point, and were compared using two-way repeated measures ANOVA (factor 1: time point; factor 2: data point) with post hoc Holm–Sidak multiple comparisons procedure.

2.5. MRI

To investigate the structural lesion caused by ET-1 injection, T2-weighted MRI was performed with all 26 animals of the behavioral study (study 2) with the help of a 4.7-T BioSpec animal scanner with a 30-cm horizontal bore magnet (Bruker BioSpin, Ettlingen, Germany). Radio frequency transmission was achieved with a Helmholtz coil (diameter: 12 cm) and the signal was detected with a 22 mm-diameter surface receiver coil, positioned above the skull of the animal. T2-weighted images were acquired with a multislice multiecho Carr-Purcell-Meiboom-Gill (CPMG) sequence: TR/TE = 4000/11.0 ms, 16 echoes, FOV = $3 \times 4\,cm^2$, slice thickness: 1.0 mm, interslice distance: 0.0 mm, matrix: 128×128. Anesthesia, control of breathing rate and body temperature were similar to the μPET scans. Images were acquired before and 24 h after ACAo, imported in VINCI, and co-registered. With the help of a threshold tool, the lesioned areas were selected and transformed to VOIs, whose volume was collected analog to the infarct volume. After 1 month, the measurement was repeated, and images were examined for structural changes (atrophy, ventricular enlargement, cysts).

2.6. Behavioral testing

We carried out several behavioral tests to measure decision-making (food-carrying task; $n = 8$ ET-1 plus 7 shams), anxiety (elevated plus maze; $n = 16$ ET-1 plus 10 shams), and spatial working memory (spontaneous alternation in the Y-maze; $n = 16$ ET-1 plus 10 shams). Rats were tested before ACAo and during the first month (from 2nd to 4th week) after ACAo.

All behavioral testing was executed during the dark phase under red light conditions (660 nm). The two testing phases required 2 weeks each, and were performed in an isolated air conditioned chamber with a controlled temperature of constantly 22 °C. After putting the rat in the test arena, the experimenter left the chamber and the behavior was digitally recorded and surveyed from outside the chamber. Food-carrying task and elevated plus maze test were then analyzed further by using a video tracking system (Ethovision 3.1, Noldus, Wageningen, Netherlands).

2.7. Food carrying task

The arena (1.5 m × 1.0 m) was a meander shaped gangway covered with a transparent plexiglas lid. It consisted of 10 interconnected straight corridors (1 m long, 15 cm wide), with a total length of 10 m. At one end of the gangway the individual home cages could be attached, so that the rats could go back and forth freely between cage and arena. During 10 days of training the rats learned to accept food in the arena. For the test, 10 pieces of food (0.5 g fruit loops, plus family) were placed in the alley. Each day, the food was presented at a different distance from cage (2–10 m in 2 m-steps, random order). Rats were tested separately once per day for 20 min or until all food was collected/eaten. Rats were digitally recorded from above, and their movement was analyzed with Ethovision (Noldus).

For offline analysis we defined a food-carrying probability score, which was assigned to each trip (=from cage to food and back). If rats carried their food all the way to the cage, this trip counted as 100% food-carrying. Those trips where rats ate their food directly at the food patch were counted as 0% food-carrying. If a rat started carrying its food to the cage but then stopped on the way to eat, the trip received a value between 0 and 100%, depending on the distance moved. For example, if the rat went 25% of the total distance toward the cage, the trip received 25% food-carrying. We calculated an average food-carrying value for each animal. In addition, we measured the number of trips, total distance moved, and velocity.

2.8. Elevated plus maze

To measure anxiety we used an elevated plus maze, a platform with two enclosed and two open arms (length: 50 cm, width: 12 cm; wall 34 cm), mounted 50 cm above ground. Rats were separately placed in the center of the maze facing one of the closed arms. Their movements were digitally recorded for 10 min and analyzed with Ethovision (Noldus). We measured the time rats spent in the different zones (open arms, enclosed arms, center) as well as the frequency of zone entry. Each rat was tested on two consecutive days and averages for each rat were calculated.

2.9. Spontaneous alternation test

We performed this test in a Y-maze with an arm length of 70 cm and a width of 13 cm. At the beginning rats were placed separately at the end of the starting arm. When the rat had entered one of the target arms and had proceeded to its end, it was taken back to its cage. The arena was cleaned thoroughly to remove all olfactory cues, and after approx. 1 min, testing was repeated. It was recorded whether the rat alternated in arm choice or went twice into the same arm. Animals were tested once per day on 3 consecutive days, and out of this the percentage of alternation was calculated.

2.10. Data analysis

Behavioral data were compared using a two-way mixed ANOVA with Tukey post hoc testing. Between-subjects factor was treatment (ET-1 and sham), within-subjects factor was time point (before and after treatment). For correlation analysis, the Pearson test was used. All percentage values were arcus sinus transformed before statistical analysis. SigmaPlot 11.0 (Systat Software, San José, CA, USA) with the integrated statistics tool SigmaStat was used for statistical analysis.

3. Results

3.1. Tolerability of ET-1 injection

We found that ET-1 and vehicle injection was well tolerated by the animals. None of the rats died during surgery or thereafter.

3.2. Study 1: ACAo model validation

3.2.1. [^{14}C]iodoantipyrine autoradiography

Quantitative [^{14}C]iodoantipyrine autoradiographic analysis revealed that after ET-1 injection, CBF was strongly reduced within the ACA territory to at least 0.02 ml/g/min after 17 min and to 0.34 ml/g/min after 2 h in the cingulate cortex (Fig. 2, columns 3 and 4). Compared to the respective values after sham (vehicle) injection, this corresponds to a mean CBF reduction of 82% (17 min) and 61% (2 h) in the cingulate cortex. A strong CBF decrease was also seen in the prelimbic cortex (on average of 72% after 17 min and of
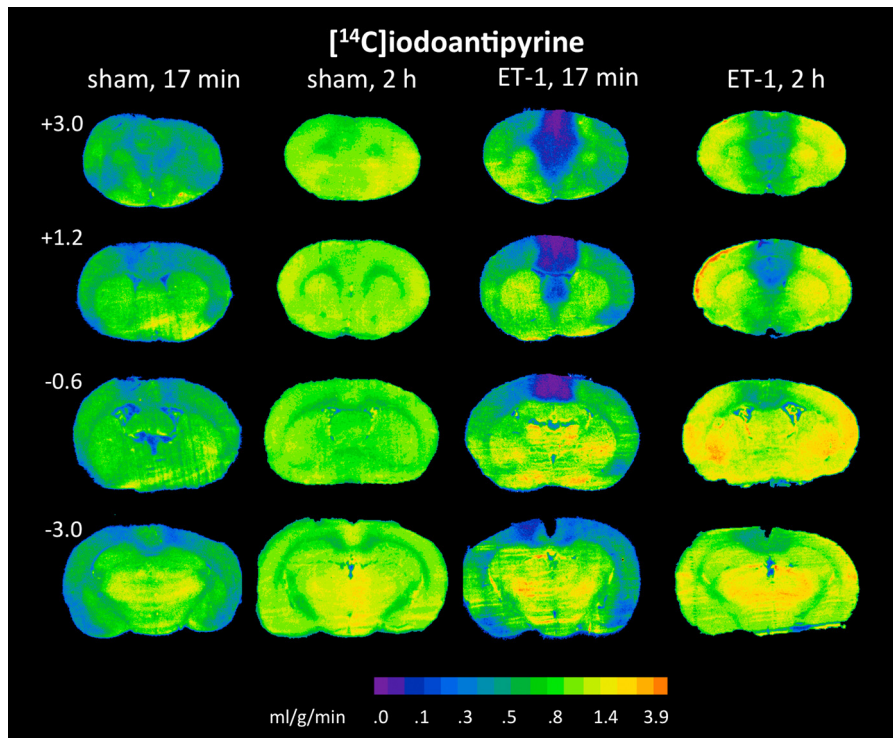
Fig. 2. Absolute CBF changes after ACAo. Quantified autoradiographic CBF images of two sham and two ET-1 injected animals. Absolute CBF 2 h after sham injection can be regarded as normal (i.e., 0.8–1.4 ml/g/min). ET-1 strongly decreased CBF in the ACA territory 17 min after injection with partial reperfusion after 2 h. Numbers on the left indicate rostrocaudal coordinates of sections with respect to Bregma.

33% after 2 h) and the secondary motor cortex M2 (on average of 49% after 17 min and 45% after 2 h). For other regional mean values see Table 1. In individual animals, CBF reduction eventually spread unilaterally into the MCA territory and affected the somatosensory cortex rather severely (minimum 0.14 ml/g/min). In most cases, these CBF reductions in the MCA territory were mild but consistently seen and remained for 2 h after ET-1 injection. This effect was most pronounced in the piriform region, where minimum perfusion was 0.32 ml/g/min after 17 min (mean CBF decrease of 11% compared to sham), and 0.71 ml/g/min after 2 h (mean CBF decrease of 30% compared to sham).

Immediately (17 min) following vehicle injection, a mild reduction of CBF was also observed in the ACA territory of sham animals (0.37 ml/g/min in the prelimbic cortex; see Fig. 2, first column) and in the MCA territory (0.38 ml/g/min in the piriform region). In contrast to ET-1 injection, however, CBF was completely restored 2 h after sham injection (1.0 and 1.5 ml/g/min; see Fig. 2, column 2). This demonstrates a transient but considerable effect on the whole cerebral cortex by the injection procedure itself.

3.2.2. Repetitive [^{15}O]H$_2$O-PET

Repetitive measurements of relative CBF (intensity normalized to cerebellum) were performed in two rats, one receiving ET-1 (5 h measurements), and the other vehicle injection (2 h measurements). After ET-1 injection, CBF was reduced in the ACA territory to <50% baseline, with the lowest values in the olfactory bulb and frontal cortex (Fig. 1). The septum was affected as well. CBF reduction peaked at the early measurements 30 min and/or 1 h after injection, and recovered thereafter slowly to baseline levels, which were reached after 4 h.

In line with the results obtained by quantitative autoradiography, a moderate CBF reduction (to >80% baseline) was observed in the MCA territory as well, particularly in the piriform cortex (Fig. 1A). This hypoperfusion could be followed by a delayed hyperperfusion in the MCA territory.

In the control animal, a moderate CBF reduction (to around 85% baseline) occurred near the vehicle injection site in the anterior part of the ACC (Fig. 1C). In the other areas, CBF changes did not exceed noise level (±10%, determined by repetitive baseline scans).

Table 1
Cerebral blood flow (mean ± standard deviation; ml/g/min) determined from [^{14}C]iodoantipyrine autoradiography. For ET-1 animals, % change compared to sham animals of the same time point is given.

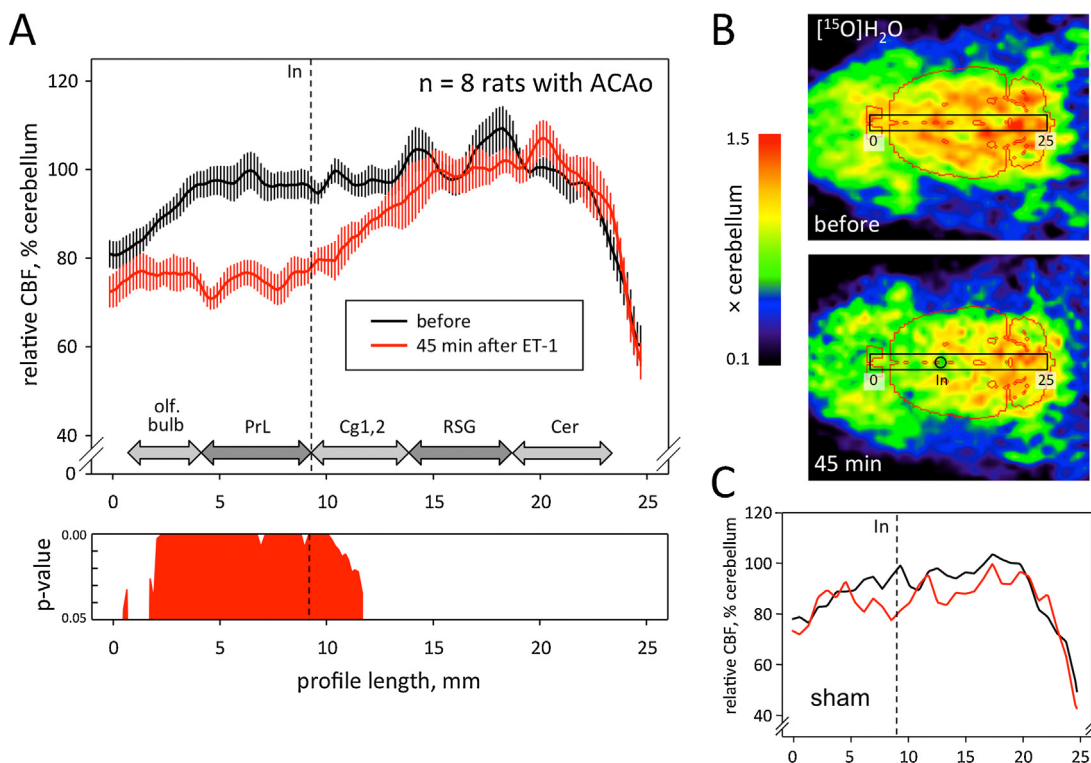| Brain area	Sham, 17 min ($n = 3$)	Sham, 2 h ($n = 2$)	ET-1, 17 min ($n = 5$)	ET-1, 2 h ($n = 3$)
Prelimbic cortex	0.50 ± 0.13	1.07 ± 0.14	0.14 ± 0.13 (−**72%**)	0.72 ± 0.27 (−**33%**)
Infralimbic cortex	0.57 ± 0.22	1.06 ± 0.08	0.26 ± 0.13 (−**54%**)	0.79 ± 0.34 (−**25%**)
Cingulate cortex Cg 1,2	0.65 ± 0.12	1.18 ± 0.10	0.12 ± 0.05 (−**82%**)	0.46 ± 0.17 (−**61%**)
Retrosplenial granular	0.85 ± 0.10	1.36 ± 0.06	0.63 ± 0.16 (−**26%**)	0.61 ± 0.22 (−**55%**)
Retrosplenial dysgranular	0.78 ± 0.09	1.27 ± 0.05	0.52 ± 0.18 (−**33%**)	0.65 ± 0.28 (−**32%**)
Motor cortex M1	0.60 ± 0.10	1.14 ± 0.02	0.56 ± 0.24 (−**7%**)	0.78 ± 0.29 (−**32%**)
Motor cortex M2	0.59 ± 0.09	1.13 ± 0.03	0.30 ± 0.13 (−**49%**)	0.62 ± 0.26 (−**45%**)
Septum	1.07 ± 0.32	1.23 ± 0.05	0.70 ± 0.40 (−**35%**)	0.96 ± 0.28 (−**22%**)
Nucl. accumbens	1.12 ± 0.37	1.35 ± 0.16	1.15 ± 0.60 (+**3%**)	1.11 ± 0.38 (−**18%**)
Caudate-putamen	1.17 ± 0.33	1.53 ± 0.07	1.52 ± 0.52 (+**30%**)	1.41 ± 0.54 (−**8%**)
Hippocampus, dorsal part	1.23 ± 0.31	1.32 ± 0.04	1.52 ± 0.39 (+**24%**)	1.25 ± 0.44 (−**5%**)
Piriform cortex	0.64 ± 0.21	1.35 ± 0.06	0.57 ± 0.28 (−**11%**)	0.95 ± 0.25 (−**30%**)

Fig. 3. Profile analysis of acute CBF changes in dorsomedial areas after ACAo. (A) Measurements of relative CBF, intensity normalized to cerebellum, were performed with $[^{15}O]H_2O$-PET at baseline (before) and 45 min after ET-1 injection. Shown are profile plots (rostral = left, caudal = right) using mean values and standard deviations over eight animals. Significant differences between the two curves are displayed below. The rostrocaudal position of the ET-1 injection site (In) is indicated by a dashed line. CBF reductions mainly occurred upstream, i.e., rostral of the injection site. (B) Single horizontal raw images of relative CBF from one animal at two time points, superimposed on a brain outline (rostral = left). The profile from which the plots in A were taken was 25 mm long and 2 mm wide and located along the brain midline. The dorsoventral position of the profile is indicated by the orange dashed line in Fig. 1D. (C) Profile plot of relative CBF taken from one of the two sham animals. A small CBF reduction around the sham injection site is visible. Abbreviations: Cer: cerebellum; Cg1,2: anterior cingulate cortex 1, 2; In: injection site; olf. bulb: olfactory bulb; PrL: prelimbic cortex; RSG: retrosplenial granular cortex.

3.3. Study 2: Behavior and regional metabolism before and after ACAo

3.3.1. Acute $[^{15}O]H_2O$-PET

CBF was measured with $[^{15}O]H_2O$ approximately 45 min after ET-1 injection ($n = 8$). The same was done with two sham-operated animals. Profile analysis demonstrated that ET-1 significantly reduced CBF around the injection site and up to 7 mm rostral to on average 70% of baseline (Fig. 3A). In the sham animals, a small zone with CBF reduction to 80% baseline could be found as well reaching approx. 3 mm rostral from the injection site (Fig. 3C). Voxel-based analysis in ET-1 animals revealed a statistically significant CBF reduction in the whole ACA territory including the septum (see t-map in Fig. 4). In lateral parts of the brain, including the piriform region, CBF changes were not significant.

3.3.2. Acute and chronic $[^{18}F]FDG$-PET

Medial profile analysis of $[^{18}F]FDG$ images after ET-1 injection revealed a decrease of relative metabolic activity. An initial reduction of FDG uptake 1 h after ET-1 injection was most prominent in the olfactory bulb (to 80% baseline; Fig. 5) and around the injection site (to 90% baseline). In the olfactory bulb, a partial recovery was apparent after one month. A delayed reduction of metabolic activity to 80% baseline occurred at the frontal pole of the brain and also caudally from the injection site after 1 month. In the sham animals, an initial metabolic reduction around the injection site, but not in the olfactory bulb, was seen as well, which was fully recovered by one month after injection. Voxel-based comparison between baseline and one month after ET-1 injection confirmed the reduction of metabolic activity in the ACA territory (Fig. 6). Furthermore, a

significant decrease of FDG uptake occurred also in lateral parts of the brain, particularly in the piriform region.

3.3.3. Structural MRI

Twenty-four hours after ET-1 injection, T2-weighted MR images revealed a hyperintense signal in the ACA territory representing structural loss and cerebral edema (Fig. 4, right column). Affected regions matched the regions of reduced blood flow visible in $[^{14}C]$iodoantipyrine autoradiography (Fig. 2, third column). Mean infarct volume calculated from the hyperintense regions was $73.5 \pm 43.4 \, mm^3$ in the 16 animals injected with ET-1. In addition, a hyperintense signal occurred in the piriform region of three animals (one unilateral, two bilateral). After 1 month, the ischemic lesion was still visible in the ET-1 injected rats (Fig. 6, right column), accompanied by ventricular enlargement and loss of tissue, particularly in midline cortex and septum. In the 10 sham operated animals, the hyperintense signal after 24 h was restricted to the injection site, comprising $2.6 \pm 5.6 \, mm^3$. After 1 month, the small edema around the injection site had disappeared completely without any signs of structural damage.

3.3.4. Behavior
3.3.4.1. Food-carrying task. ACAo reduced food-carrying scores from $86 \pm 25\%$ before ET-1 injection to $60 \pm 42\%$ after 1 month (Fig. 7A). In the seven control rats, food-carrying remained constant at $73 \pm 28\%$ before and $72 \pm 31\%$ after sham injection. However, there were neither significant main effects of treatment or time point, nor a significant factor interaction. Because of the high standard deviations of both food carrying after ACAo and of infarct volume, we performed a correlation analysis between the two
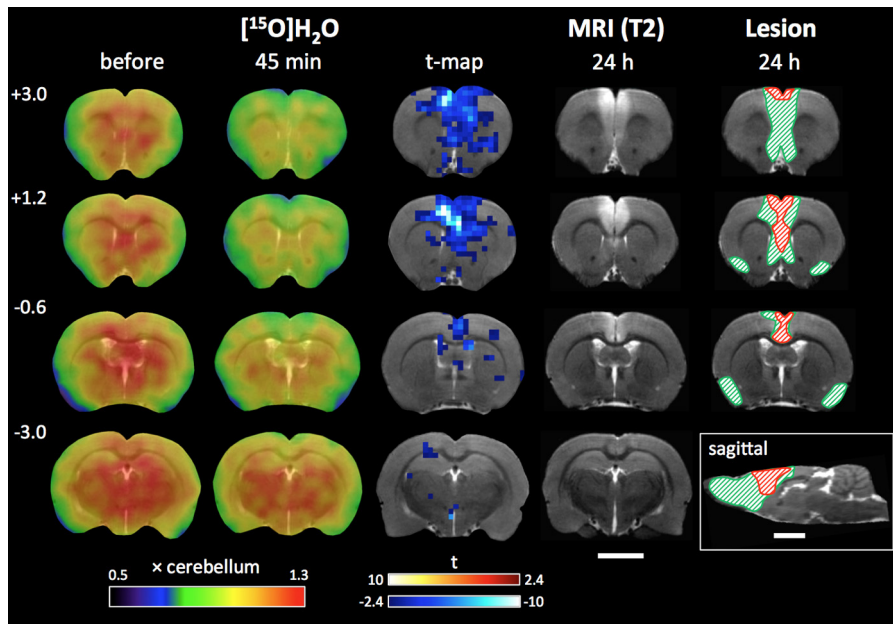
Fig. 4. Voxel-based analysis of acute CBF changes and structural lesions after ACAo. Mean relative CBF values (intensity normalized to cerebellum) from the same eight animals as shown in Fig. 3, projected onto an MRI template, before (first column) and 45 min after ET-1 injection (second column). The third column shows the respective t-map, resulting from a voxel-based paired t-test. Critical t-values were ±2.4, and only significant changes ($p < 0.05$, uncorrected) are displayed. The presence of solely blue-colored voxels indicates that 45 min after ACAo only hypoperfusion occurred. Forth column: T2-weighted MR images of one single animal taken 24 h after ACAo. The location of the edema (hyperintensity) matches the area of severely reduced CBF (see also Fig. 2, third column, purple color). The fifth column displays maximal (green) and minimal (red) structural lesions in three transverse and one sagittal section. Scale bars: 5 mm.
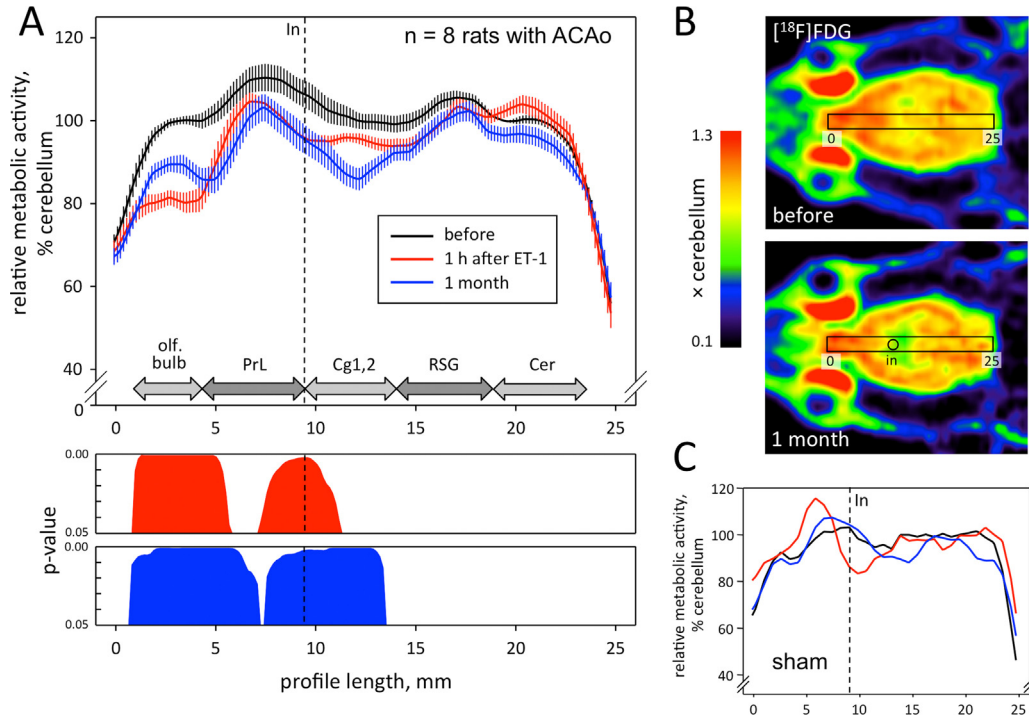

Fig. 5. Profile analysis of longitudinal metabolic changes in dorsomedial areas after ACAo. (A) Measurements of relative metabolic activity, intensity normalized to cerebellum, were performed with [¹⁸F]FDG-PET in the same eight animals as shown in Fig. 3. Time points were baseline (before), 1 h and 1 month after ET-1 injection. Profile plots are mean values and standard deviations, and significant differences between baseline and post-ACAo time points are shown below. Metabolic activity most strongly decreased in the olfactory bulb and the anterior cingulate cortex. (B) Single horizontal raw images (anterior is left) of relative metabolic activity from one animal before and 1 month after ET-1 injection, together with the localization of the profile. (C) Profile plot of relative metabolic activity taken from one of the sham animals. 1 h after ET-1 injection, there was a decrease of metabolic activity around the injection site (In), and an increase rostral from it (red line). After one month (blue line), metabolic activity was similar to baseline (black line). Abbreviations: Cer: cerebellum; Cg1,2: anterior cingulate cortex 1, 2; In: injection site; olf. bulb: olfactory bulb; PrL: prelimbic cortex; RSG: retrosplenial granular cortex.
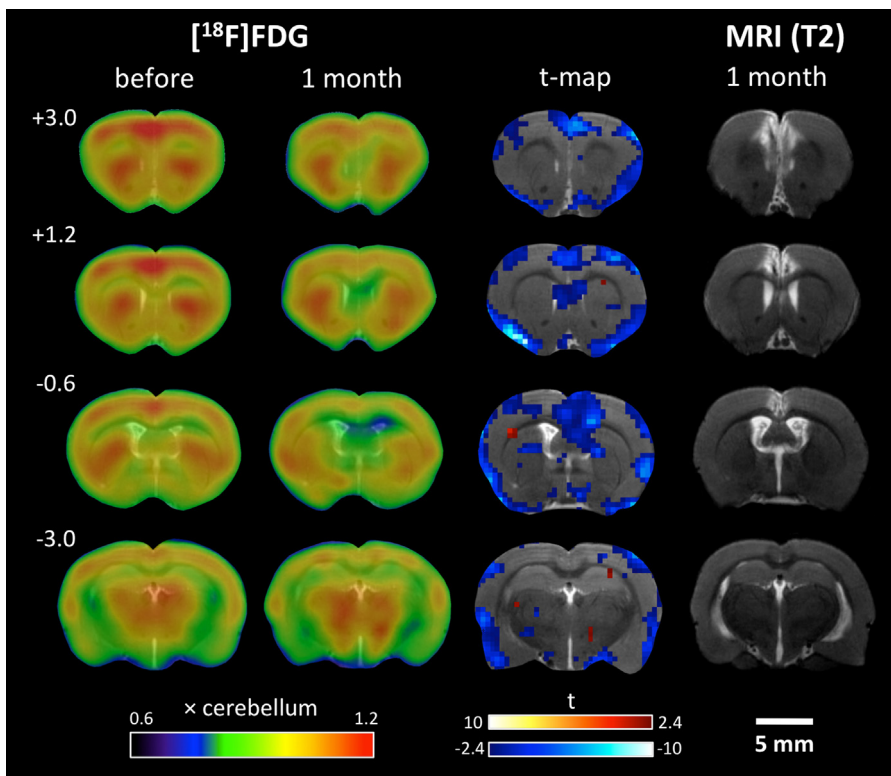
Fig. 6. Voxel-based analysis of longitudinal metabolic changes after ACAo. Mean relative metabolic activity (FDG-uptake normalized to cerebellum) from the same eight animals as shown in Fig. 3, projected onto an MRI template, before (first column) and 1 month after ET-1 injection (second column). The third column shows the respective *t*-map, resulting from a voxel-based paired *t*-test. Critical *t*-values were ±2.4, and only significant changes ($p < 0.05$, uncorrected) are displayed. Hypometabolism was present in the ACA territory, but also in the lateral cortex, particularly the insular and piriform region. Forth column: T2-weighted MR images of one single animal (the same rat as shown in Fig. 4) taken 1 month after ACAo. The former edema has developed into a structural lesion (hyperintense region), accompanied by ventricular enlargement.
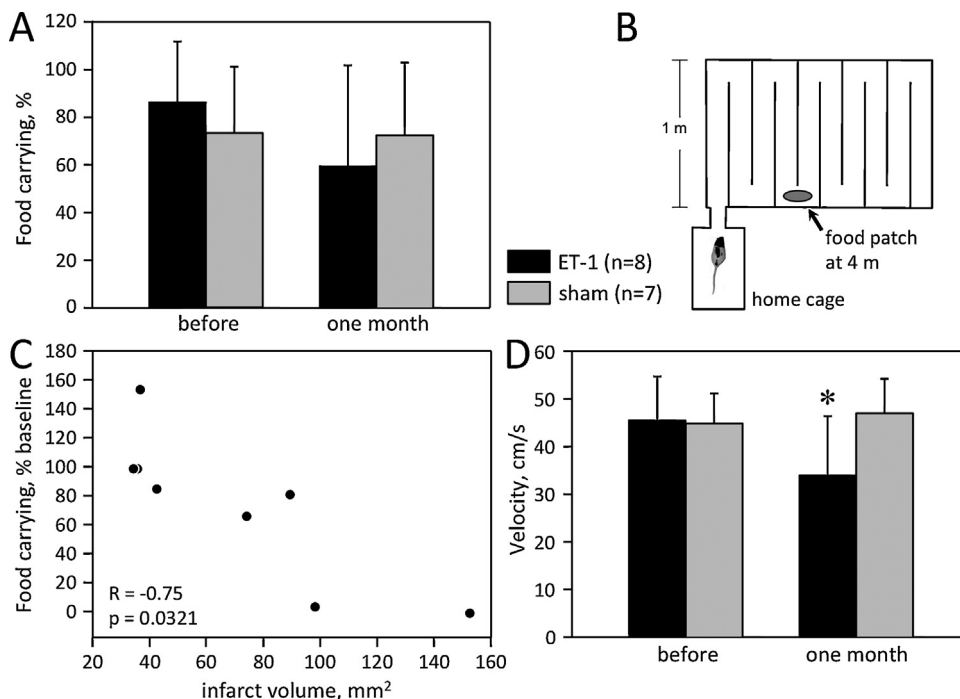

Fig. 7. Changes of food-carrying behavior after ACAo. Food-carrying was tested with the eight ACAo and two sham rats from the PET study, plus five additional sham animals. (A) Mean food-carrying probability with standard deviations. There were no significant differences between groups or time points. (B) Schematic drawing of the meander-shaped arena (total length of walkway: 10 m) with home cage attached. Location of the food patch varied randomly across sessions, in this example it was located at 4 m distance from cage. (C) Correlation between change in food-carrying probability and infarct volume indicates a contribution of ACA territory areas to the food-handling decision. (D) Mean food-carrying velocity with standard deviations. After 1 month, ACAo rats were significantly slower than sham animals.
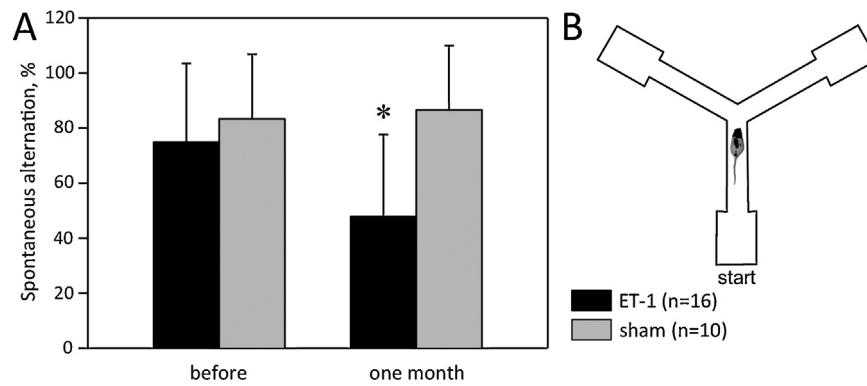
Fig. 8. Changes of spontaneous alternation after ACAo. This test was carried out with the 10 animals from the PET study plus 16 additional rats, resulting in 16 ACAo and 10 sham animals. (A) Spontaneous alternation rate (mean and standard deviation) significantly decreased 1 month after ET-1 injection, indicating impaired spatial working memory. (B) Schematic drawing of the Y-maze.

variables. We found a significant negative correlation ($R = -0.75$; $p = 0.0321$; Fig. 7C), indicating that the bigger the infarct, the lower food-carrying probability.

Food-carrying probability was influenced by distance between food and home-cage ($F(4,52) = 3.64$; $p = 0.0109$) before ET-1/sham injection, with 2 m distance having a higher probability for food-carrying than 8 m and 10 m ($p < 0.05$). However, post hoc comparisons separately performed for sham and ACAo groups revealed that this effect was significant in the sham group only, and disappeared after ET-1/sham injection ($F(4,52) = 2.22$; $p = 0.08$).

Food-carrying velocity (Fig. 7D) was reduced after ACAo from 46 ± 9 cm/s before to 34 ± 12 cm/s after 1 month. In control animals, velocity was not decreased after sham injection (45 ± 6 cm/s before, 47 ± 7 cm/s after injection). While main effects of factors treatment and time point were not significant, there was a significant factor interaction ($F(1,13) = 5.56$; $p = 0.0348$). Post hoc testing revealed a significant difference between velocity of ET-1 injected animals before versus after ACAo, as well as a significant difference between velocity of ET-1 versus sham rats after injection ($p < 0.05$).

ACAo reduced the number of trips from 36 ± 12 to 25 ± 12. In sham animals, the number of trips was reduced as well, from 33 ± 11 to 27 ± 10. There was a significant main effect of time point ($F(1,13) = 5.97$; $p = 0.0296$), and post hoc testing showed a significant difference of the number of trips before versus after injection in the ET-1 group ($p < 0.05$). Consequently, the total distance moved was reduced as well from 406 ± 86 m before ACAo to 293 ± 97 m after one month in ET-1 rats, and from 373 ± 94 m to 294 ± 55 in sham animals. Factor time point had a significant main effect on total distance moved ($F(1,13) = 11.59$; $p = 0.0047$), and post hoc testing revealed a significant difference of total distance moved before versus after ET-1 injection ($p < 0.05$).

3.3.4.2. Spontaneous alternation. ACAo reduced spontaneous alternation from $75 \pm 28\%$ before to $48 \pm 30\%$ after ET-1 injection (Fig. 8). In control animals, spontaneous alternation remained high: $83 \pm 24\%$ before and $87 \pm 23\%$ after sham injection. ANOVA revealed a significant main effect of treatment ($F(1,24) = 6.24$; $p = 0.0197$), and a significant factor interaction ($F(1,24) = 8.14$; $p = 0.0088$). Within the ET-1 group there was a significant difference between before and after ACAo ($p < 0.05$), and at time point "after injection" there was a significant difference between the ET-1 and sham group ($p < 0.05$).

3.3.4.3. Elevated plus maze. ACAo increased open arm time (% of total time) and open arm entries (% of total zone entries), indicating decreased anxiety. Open arm time increased from $35 \pm 19\%$ to $57 \pm 15\%$, and open arm entries from $24 \pm 8\%$ to $35 \pm 6\%$ (Fig. 9A and C). In sham animals, both variables increased only slightly,

open arm time from $41 \pm 14\%$ to $49 \pm 9\%$, and open arm entries from $27 \pm 5\%$ to $29 \pm 6\%$. Time point had a significant main effect on both open arm time ($F(1,24) = 8.30$; $p = 0.0082$) and open arm entries ($F(1,24) = 9.49$; $p = 0.0051$) with a significant difference between before and after injection in the ET-1 group ($p < 0.05$).

The total frequency of zone entries, which represents a measure for exploratory activity, increased in ET-1 animals after 1 month from 79 ± 35 to 126 ± 47. In control rats it remained constant at 103 ± 37 zone entries before and 102 ± 22 after sham injection (Fig. 9D). Factor time point had a significant main effect on zone entries ($F(1,24) = 6.94$; $p = 0.0145$), and there was a significant factor interaction ($F(1,24) = 7.31$; $p = 0.0124$). In the ET-1 group, number of zone entries was significantly higher after 1 month than before ACAo ($p < 0.05$).

In contrast to the decrease of food-carrying velocity that was found after ACAo, walking speed in the elevated plus maze increased from 16 ± 3 cm/s to 23 ± 9 cm/s on the open arms, and from 16 ± 3 cm/s to 22 ± 5 cm/s on the closed arms. In sham animals, velocity remained constant at 12 ± 5 cm/s before and 11 ± 4 cm/s after sham injection on the open arms, and at 13 ± 4 cm/s before and 12 ± 4 cm/s after sham injection on the closed arms. Treatment had a significant main effect on velocity both on the open ($F(1,23) = 21.23$; $p = 0.0001$) and closed arms ($F(1,24) = 26.79$; $p < 0.0001$), while factor time point significantly influenced velocity on closed arms only ($F(1,24) = 6.45$; $p = 0.018$). For both open and closed arms there was a significant factor interaction ($F(1,23) = 5.77$; $p = 0.0248$ for open arms; $F(1,24) = 7.72$; $p = 0.104$ for closed arms). Post hoc comparison revealed that animals of the ACAo group were significantly faster after ET-1 injection than before, on both open and closed arms ($p < 0.05$). Furthermore, 1 month after injection velocity was significantly higher in the ACAo group compared to sham group for both open and closed arms ($p < 0.05$).

4. Discussion

4.1. Changes of perfusion after ACAo (study 1 and 2)

In the acute phase after injection of the vasoconstrictor ET-1, repetitive [^{15}O]H$_2$O-PET demonstrated the course of CBF reduction for up to 2 h and subsequent recovery with normalization after approximately 4 h. CBF reduction was highest and lasted longest in the anterior cingulate cortex. Other regions of the ACA territory, some of them located rostral to the ET-1 injection site, were affected as well, but were reperfused somewhat earlier. Rostral vasoconstriction was most likely mediated by ACA branches, which originate near the injection site, and run in an anterodorsal direction (see Fig. 1). In addition, upstream vasoconstriction may have
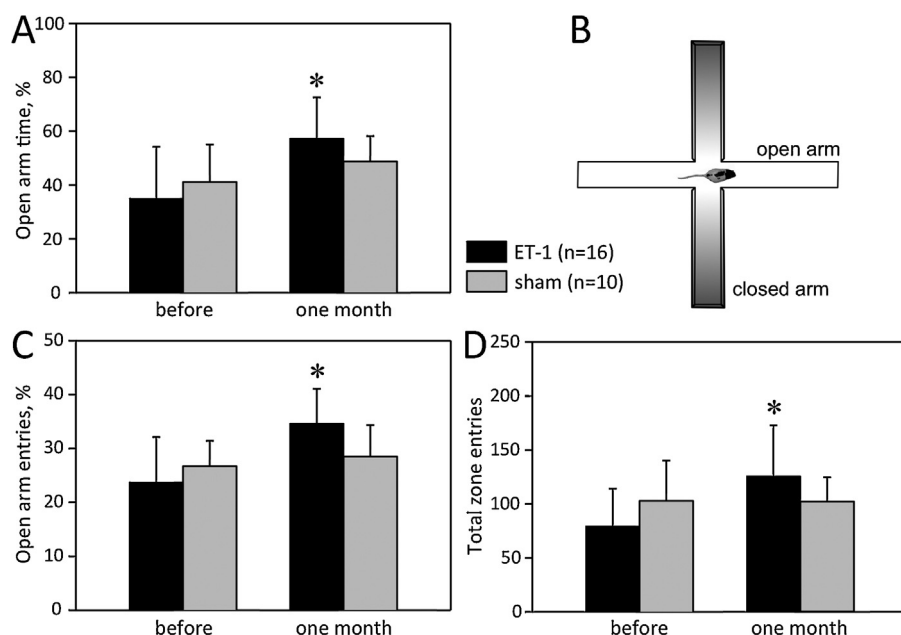
Fig. 9. Changes of elevated plus maze behavior after ACAo. This test was carried out with 16 ACAo and 10 sham animals. (A) Relative open arm time (% of total time; mean and standard deviation) significantly increased one month after ET-1 injection, indicating decreased anxiety. (B) Schematic drawing of the elevated plus maze. (C) Relative open arm entries (% of total zone entries) significantly increased 1 month after ET-1 injection, confirming reduced anxiety. (D) The absolute number of total zone entries significantly increased after ACAo, indicating increased exploratory activity.

contributed as well, caused by ET-1 diffusion along the ACA or by conducted vasoconstriction due to upstream signaling (Gustafsson and Holstein-Rathlou, 1999). Compared to the study of Ward et al. (Ward et al., 1998) we injected ET-1 at a more distal segment of the ACA, approximately at the border between prelimbic cortex and anterior cingulate cortex. This explains why other, more proximally located regions like the nucleus accumbens, olfactory tubercle and diagonal band of Broca have not been affected in our study. ET-1 has been used in other stroke models to produce infarcts in the MCA territory or lacunar infarcts in rats (Cordova et al., 2014; Fuxe et al., 1997; Joo et al., 2012; Livingston-Thomas et al., 2013; Roome et al., 2014), mice (Soylu et al., 2012), and marmosets (Virley et al., 2004), with the duration of CBF reduction being comparable to our results.

Quantitative [^{14}C]iodoantipyrine autoradiography revealed that CBF was reduced to less than 0.1 ml/g/min (<10% baseline) 17 min after ET-1 injection. This is in line with studies investigating early ET-1 action and showing that vasoconstriction is maximal during the first 15–30 min after injection (Nikolova et al., 2009; Regenhardt et al., 2013). Subsequently, blood vessels slowly begin to dilate, depending on local ET-1 concentration. This may explain why our earliest [^{15}O]H$_2$O-PET measurements performed at 30 min after ET-1 injection merely showed a CBF reduction to 70% baseline.

4.2. Metabolic changes after ACAo (study 2)

For interpretation of [^{18}F]FDG-PET results we have to keep in mind that FDG uptake took place under anesthesia, where cortico-cortical as well as thalamo-cortical networks are severely altered (Bonhomme et al., 2012) and glucose metabolism is strongly decreased, particularly in thalamus and cortex (Prieto et al., 2011). Glutamatergic excitatory activity, which accounts for 80% of the brain's energy consumption in the awake state (Raichle and Mintun, 2006), is reduced during isoflurane anesthesia so that FDG uptake presumably reflects for the most part inhibitory activity, basic housekeeping functions (e.g., protein trafficking), and possibly activation of the adrenergic system (Boretius et al., 2013). The "metabolic lesions" observed in the ACA territory and elsewhere

therefore represent mainly general loss of brain cells as well as disturbance of the inhibitory part of functional brain networks. Profile analysis of [^{18}F]FDG-PET starting 1 h after ET-1 injection showed substantial metabolic reduction in the olfactory bulb, but not in the other areas of reduced CBF. This may be explained by the fact that in ischemic tissue with some residual blood flow FDG influx can be normal or even elevated 1 h after occlusion, because reduced glucose supply is compensated for by increased glucose phosphorylation (Backes et al., 2011; Walberer et al., 2012). After 1 month, FDG uptake had recovered in the olfactory bulb. This may result at least to some extent from neuronal progenitor cell traveling with the rostral migratory stream from the subventricular zone to the olfactory bulb (Liu and Guthrie, 2011). However, since migration is very slow (the full journey takes at least 75 days; (Whitman and Greer, 2009)) and only interneurons are replaced (Liu and Guthrie, 2011), other mechanisms must have contributed to metabolic recovery. In contrast to the olfactory bulb, FDG uptake was further decreased in the anterior cingulate cortex, prelimbic/infralimbic cortex, and septum, reflecting loss of tissue as confirmed by MRI.

Voxel-based analysis showed that a significant decrease of relative metabolic activity did not only occur in the ACA territory, but also in lateral cortical regions, particularly in the piriform area. Furthermore, a piriform hyperintense signal was found in structural MR images 24 h after ET-1 injection in three animals. There was no significant CBF reduction detectable with [^{15}O]H$_2$O-PET in this area of the same animals 45 min after ACAo, although IAP autoradiography with other rats has indicated that this can indeed occur, as described for human stroke patients (Rubin et al., 2000). The metabolic reduction in the piriform region therefore may reflect a remote, diaschisis-like effect that is presumably independent of CBF changes. Diaschisis is a phenomenon related to all kinds of focal brain lesions, where impairments can spread to remote areas functionally connected to the original site of damage (Finger et al., 2004). The rat piriform cortex is reciprocally connected to the prelimbic and infralimbic region, fulfilling in our case the anatomical prerequisite of diaschisis (Datiche and Cattarelli, 1996; Heidbreder and Groenewegen, 2003; Johnson et al., 2000). In MCA stroke patients crossed cerebellar

diaschisis is common, leading to chronic reduction of FDG uptake in the contralateral cerebellum (Agrawal et al., 2011; Shih et al., 2006). Acute and subacute studies of transhemispheric cortical diaschisis after MCAo report transient contralesional hyperexcitability with increased FDG uptake upon sensory stimulation during the first week (Mohajerani et al., 2011). However, this does not result in chronic hypometabolism, and is interpreted as circuit remodeling in the course of functional compensation by the contralateral cortical area (Takatsuru et al., 2009). One mechanism underlying hyperexcitability during transhemispheric diaschisis is the breakdown of inhibitory synaptic transmission (Imbrosci et al., 2014), which may cause excitotoxicity and death of neurons in susceptible areas. Interestingly, both cerebellum and piriform cortex are selectively vulnerable to excitotoxicity (Candelario-Jalil et al., 2001; Welsh et al., 2002). We therefore conclude that hypometabolism in midline brain areas after ACAo is caused by the ischemic lesion, while reduced FDG uptake in lateral cortical regions is related to diaschisis-like phenomena.

4.3. Effect of ACAo on decision-making during foraging

In order to test alterations of decision-making strategies in rats, we used a food-carrying task whose basic principles were developed more than 60 years ago (Bindra, 1948; Morgan, 1947; Wolfe, 1939). The rat encounters food in a meander-shaped arena and has two alternatives, namely carrying the food back to the cage or eating it directly at the food patch (Whishaw et al., 1990). This is reflected by the food-carrying probability score, which was inversely correlated to infarct size, suggesting that areas of the ACA territory are involved in the food-handling decision. This is in line with other studies implicating anterior cingulate cortex and nucleus accumbens in foraging strategies (Whishaw and Kornelsen, 1993; Li et al., 2012). Closely associated with food-carrying probability was the number of food-carrying trips, total distance moved, and walking speed, which were all significantly reduced after ACAo, but not after sham operation. We can therefore conclude that food-handling decisions had changed after ACAo favoring less motor activity. It is unlikely that this was caused by a disturbance of the primary motor system, since the same animals showed increased walking speed on the elevated plus maze (see below). However, ischemic lesions in the secondary motor cortex M2 may have contributed to behavioral changes, since M2 neurons are involved in self-initiated actions (Murakami et al., 2014).

Several factors influence the food-handling decision, including emotional parameters as shyness, fear, and anxiety (Dringenberg et al., 1994, 2000). To test anxiety in our rats we used the elevated plus maze test, where animals can move freely between two enclosed and two open arms of an elevated platform. Relative open arm time and relative number of open arm entries are inverse measures of anxiety, whereas the total number of zone entries reflects exploratory activity (Doremus et al., 2006; Rodgers and Johnson, 1995). Both open arm time and open arm entries increased 1 month after ACAo, but remained constant in sham animals, suggesting that after ACAo, animals were less anxious than before. This is in line with findings emphasizing the role of the orbitofrontal-infralimbic/prelimbic-amygdala network (Rempel-Clower, 2007; Sotres-Bayon and Quirk, 2010) and also the cingulate cortex (Albrechet-Souza et al., 2009; Maier et al., 2012) and nucleus accumbens (Yorgason et al., 2013) for anxiety-like behavior. Our findings therefore suggest that at least part of the reduction of food-carrying and walking speed may be attributed to a decrease of anxiety directly caused by the focal ischemic lesion.

Distance between food and refuge is another important factor for the food-handling decision. Long distances lead to extended travel times in case of food-carrying, which may be worthwhile only when food eating time is also long (Whishaw et al., 1990;

Nakatsuyama and Makino, 1999; Whishaw and Dringenberg, 1991; Whishaw and Tomie, 1989). Particularly these economic factors have been investigated in relation to optimal foraging theory (Whishaw and Dringenberg, 1991; Lima et al., 1985; Phelps and Roberts, 1989; Whishaw, 1990), which describes the trade-off between predatory risk and energy gain (Cezilly and Benhamou, 1996; Pyke, 1984; Pyke et al., 1977). For a correct decision in terms of optimal foraging theory it is necessary that the rat is aware of its location and able to estimate travel time. Therefore, navigational skills have been investigated with the food-carrying task as well, including sensory hierarchy and cue competition during piloting and dead reckoning (Gibson and Shettleworth, 2003; Maaswinkel and Whishaw, 1999; Tigner and Wallace, 1972; Whishaw and Tomie, 1997). We have used the spontaneous alternation test to obtain a crude measure of spatial working memory. Spontaneous alternation was reduced after ACAo, but not after sham operation. However, alternation behavior depends not only on spatial working memory, but also on the animal's willingness to explore a novel environment (Hughes, 2004; Lalonde, 2002). Our results from elevated plus maze testing had demonstrated that anxiety had decreased after ET-1 injection, while exploratory activity had increased (see above). We can therefore conclude that reduction of spontaneous alternation to chance level after ACAo reflects a decrease of spatial memory rather than neophobia. A loss of spatial memory may therefore have contributed to the decrease of food-carrying after ACAo. However, the fact that distance between food and cage had no significant effect on the food-carrying decision in the ACAo-group even before ET1-injection suggests that this contribution may be small.

An unexpected finding was that walking speed during food-carrying decreased from 46 to 34 cm/s after ACAo, while walking speed on the elevated plus maze increased from 16 to 23 cm/s (open arms) or 22 cm/s (closed arms), respectively. This illustrates one of the main findings of this study, namely that ACAo indeed changes behavior, but not in a generalized fashion resulting in either hypoactivity (apathy, passivity) or hyperactivity (agitation). Rather, behavioral changes seem highly context-dependent. In the food-carrying task, rats leave their home-cage voluntarily to forage, and run back to their refuge at high speed after they have decided to carry their food. The motivation to carry and to move fast may be anxiety, which functions to move the animal toward danger using appropriate risk assessment behavior (McNaughton and Corr, 2004). After ACAo, this motivational factor may be reduced, resulting in less food-carrying with lower walking speed. On the elevated plus maze, however, there is no refuge and no food, so that goal-directed behavior cannot develop. In the absence of a task, the effects of ACAo shift toward hyperactivity, with the animal restlessly roaming the maze. In a similar fashion, a mixture of apathy and agitation occurs in the majority of institutionalized dementia patients (Buettner and Fitzsimmons, 2006), whereby a decrease of gray matter density in the anterior cingulate cortex correlates with the severity of both behavioral states (Bruen et al., 2008). In ACAo patients (stroke or ruptured aneurysms) apathy predominates, but agitation is observed as well (Kumral et al., 2002; Kang and Kim, 2008). That even severe abulia is highly context-dependent has been impressively shown by the telephone effect (Fisher, 1983), where mute patients can be tricked into animated talking by calling them on the phone.

5. Conclusions

Taken together, our results show that stereotactic injection of ET-1 induces vasoconstriction long enough to induce bilateral ischemic infarction in the ACA territory in rats. ACAo in the early chronic stage, i.e., 1 month after ET-1 injection, decreased food-carrying behavior and walking speed in a foraging situation, which

can be explained by decreased anxiety. Spatial working memory decreased as well, but seemed to be less important for the food-handling decision. While reduced activity during goal-directed behavior develops analog to executive impairments and abulia in human ACAo patients, the same rats show increased exploratory activity and restlessness in the absence of task-related stimuli. We conclude that the rat ACAo model is not only suitable to study the effects of ACA stroke with respect to functional deterioration and recovery, but also to investigate how stroke symptoms are provoked or alleviated by environment and context.

Conflict of interest

There is no conflict of interest to declare.

References

Agrawal KL, Mittal BR, Bhattacharya A, Khandelwal N, Prabhakar S. Crossed cerebellar diaschisis on F-18 FDG PET/CT. Indian J Nucl Med 2011;26:102–3.

Albrechet-Souza L, Borelli KG, Carvalho MC, Brandão ML. The anterior cingulate cortex is a target structure for the anxiolytic-like effects of benzodiazepines assessed by repeated exposure to the elevated plus maze and Fos immunoreactivity. Neuroscience 2009;164:387–97.

Arboix A, Garcia-Eroles L, Sellares N, Raga A, Oliveres M, Massons J. Infarction in the territory of the anterior cerebral artery: clinical study of 51 patients. BMC Neurol 2009;9:30.

Backes H, Walberer M, Endepols H, Neumaier B, Graf R, Wienhard K, et al. Whiskers area as extracerebral reference tissue for quantification of rat brain metabolism using 18F-FDG PET: application to focal cerebral ischemia. J Nucl Med 2011;52:1252–60.

Bindra D. What makes rats hoard. J Comp Physiol Psych 1948;41:397–402.

Bird CM, Castelli F, Malik O, Frith U, Husain M. The impact of extensive medial frontal lobe damage on 'Theory of Mind' and cognition. Brain 2004;127:914–28.

Bogousslavsky J. Frontal stroke syndromes. Eur Neurol 1994;34:306–15.

Bogousslavsky J, Regli F. Anterior cerebral artery territory infarction in the Lausanne Stroke Registry Clinical and etiologic patterns. Arch Neurol 1990;47:144–50.

Bonhomme V, Boveroux P, Brichant JF, Laureys S, Boly M. Neural correlates of consciousness during general anesthesia using functional magnetic resonance imaging (fMRI). Arch Ital Biol 2012;150:155–63.

Boretius S, Tammer R, Michaelis T, Brockmoller J, Frahm J. Halogenated volatile anesthetics alter brain metabolism as revealed by proton magnetic resonance spectroscopy of mice in vivo. Neuroimage 2013;69:244–55.

Böttger S, Prosiegel M, Steiger HJ, Yassouridis A. Neurobehavioural disturbances, rehabilitation outcome, and lesion site in patients after rupture and repair of anterior communicating artery aneurysm. J Neurol Neurosurg Psychiatry 1998;65:93–102.

Bruen PD, McGeown WJ, Shanks MF, Venneri A. Neuroanatomical correlates of neuropsychiatric symptoms in Alzheimer's disease. Brain 2008;131:2455–63.

Buettner L, Fitzsimmons S. Mixed behaviors in dementia: the need for a paradigm shift. J Gerontol Nurs 2006;32:15–22.

Candelario-Jalil E, Al-Dalain SM, Castillo R, Martinez G, Fernandez OS. Selective vulnerability to kainate-induced oxidative damage in different rat brain regions. J Appl Toxicol 2001;21:403–7.

Cezilly F, Benhamou S. Optimal foraging strategies: a review. Rev Ecol Terre Vie 1996;51:43–86.

Cordova CA, Jackson D, Langdon KD, Hewlett KA, Corbett D. Impaired executive function following ischemic stroke in the rat medial prefrontal cortex. Behav Brain Res 2014;258:106–11.

Datiche F, Cattarelli M. Reciprocal and topographic connections between the piriform and prefrontal cortices in the rat: a tracing study using the B subunit of the cholera toxin. Brain Res Bull 1996;41:391–8.

Doremus TL, Varlinskaya EI, Spear LP. Factor analysis of elevated plus-maze behavior in adolescent and adult rats. Pharmacol Biochem Behav 2006;83:570–7.

Dringenberg HC, Kornelsen RA, Vanderwolf CH. Food carrying in rats is blocked by the putative anxiolytic agent buspirone. Pharmacol Biochem Behav 1994;49:741–6.

Dringenberg HC, Wightman M, Beninger RJ. The effects of amphetamine and raclopride on food transport: possible relation to defensive behavior in rats. Behav Pharmacol 2000;11:447–54.

Feigin VL, Forouzanfar MH, Krishnamurthi R, Mensah GA, Connor M, Bennett DA, et al. Global and regional burden of stroke during 1990–2010: findings from the Global Burden of Disease Study 2010. Lancet 2014;383:245–54.

Finger S, Koehler PJ, Jagella C. The Monakow concept of diaschisis: origins and perspectives. Arch Neurol 2004;61:283–8.

Fisher CM. Honored guest presentation: abulia minor vs agitated behavior. Clin Neurosurg 1983;31:9–31.

Fuxe K, Bjelke B, Andbjer B, Grahn H, Rimondini R, Agnati LF. Endothelin-1 induced lesions of the frontoparietal cortex of the rat. A possible model of focal cortical ischemia. Neuroreport 1997;8:2623–9.

Gacs G, Fox AJ, Barnett HJ, Vinuela F. Occurrence and mechanisms of occlusion of the anterior cerebral artery. Stroke 1983;14:952–9.

Gibson BM, Shettleworth SJ. Competition among spatial cues in a naturalistic food-carrying task. Learn Behav 2003;31:143–59.

Gustafsson F, Holstein-Rathlou N. Conducted vasomotor responses in arterioles: characteristics, mechanisms and physiological significance. Acta Physiol Scand 1999;167:11–21.

Heidbreder CA, Groenewegen HJ. The medial prefrontal cortex in the rat: evidence for a dorso-ventral distinction based upon functional and anatomical characteristics. Neurosci Biobehav Rev 2003;27:555–79.

Hossmann KA. Viability thresholds and the penumbra of focal ischemia. Ann Neurol 1994;36:557–65.

Hughes RN. The value of spontaneous alternation behavior (SAB) as a test of retention in pharmacological investigations of memory. Neurosci Biobehav Rev 2004;28:497–505.

Hütter BO, Gilsbach JM. Cognitive deficits after rupture and early repair of anterior communicating artery aneurysms. Acta Neurochir (Wien) 1992;116:6–13.

Imbrosci B, Ytebrouck E, Arckens L, Mittmann T. Neuronal mechanisms underlying transhemispheric diaschisis following focal cortical injuries. Brain Struct Funct 2014 [in press].

Johnson DM, Illig KR, Behan M, Haberly LB. New features of connectivity in piriform cortex visualized by intracellular injection of pyramidal cells suggest that primary olfactory cortex functions like association cortex in other sensory systems. J Neurosci 2000;20:6974–82.

Joo HW, Hyun JK, Kim TU, Chae SH, Lee YI, Lee SJ. Influence of constraint-induced movement therapy upon evoked potentials in rats with cerebral infarction. Eur J Neurosci 2012;36:3691–7.

Kang SY, Kim JS. Anterior cerebral artery infarction: stroke mechanism and clinical-imaging study in 100 patients. Neurology 2008;70:2386–93.

Kumral E, Bayulkem G, Evyapan D, Yunten N. Spectrum of anterior cerebral artery territory infarction: clinical and MRI findings. Eur J Neurol 2002;9:615–24.

Lalonde R. The neurobiological basis of spontaneous alternation. Neurosci Biobehav Rev 2002;26:91–104.

Li F, Li M, Cao W, Xu Y, Luo Y, Zhong X, et al. Anterior cingulate cortical lesion attenuates food foraging in rats. Brain Res Bull 2012;88:602–8.

Lima SL, Valone TJ, Caraco T. Foraging-efficiency predation-risk trade-off in the grey squirrel. Anim Behav 1985;33:155–65.

Liu H, Guthrie KM. Neuronal replacement in the injured olfactory bulb. Exp Neurol 2011;228:270–82.

Livingston-Thomas JM, Hume AW, Doucette TA, Tasker RA. A novel approach to induction and rehabilitation of deficits in forelimb function in a rat model of ischemic stroke. Acta Pharmacol Sin 2013;34:104–12.

Maaswinkel H, Whishaw IQ. Homing with locale, taxon, and dead reckoning strategies by foraging rats: sensory hierarchy in spatial navigation. Behav Brain Res 1999;99:143–52.

Maier S, Szalkowski A, Kamphausen S, Perlov E, Feige B, Blechert J, et al. Clarifying the role of the rostral dmPFC/dACC in fear/anxiety: learning, appraisal or expression? PLoS ONE 2012;7:e50120.

Martinaud O, Perin B, Gerardin E, Proust F, Bioux S, Gars DL, et al. Anatomy of executive deficit following ruptured anterior communicating artery aneurysm. Eur J Neurol 2009;16:595–601.

McNaughton N, Corr PJ. A two-dimensional neuropsychology of defense: fear/anxiety and defensive distance. Neurosci Biobehav Rev 2004;28:285–305.

Mohajerani MH, Aminoltejari K, Murphy TH. Targeted mini-strokes produce changes in interhemispheric sensory signal processing that are indicative of disinhibition within minutes. Proc Natl Acad Sci U S A 2011;108:E183–91.

Morgan CT. The hoarding instinct. Psychol Rev 1947;54:335–41.

Murakami M, Vicente MI, Costa GM, Mainen ZF. Neural antecedents of self-initiated actions in secondary motor cortex. Nat Neurosci 2014., http://dx.doi.org/10.1038/nn.3826 [Epub ahead of print].

Nagaratnam N, Davies D, Chen E. Clinical effects of anterior cerebral artery infarction. J Stroke Cerebrovasc Dis 1998;7:391–7.

Nagaratnam N, Nagaratnam K, Ng K, Diu P. Akinetic mutism following stroke. J Clin Neurosci 2004;11:25–30.

Nakatsuyama E, Makino J. Food carrying determined by eating time of a food in rats (Rattus norvegicus). Psychobiology 1999;27:133–4.

Nikolova S, Moyanova S, Hughes S, Bellyou-Camilleri M, Lee TY, Bartha R. Endothelin-1 induced MCAO: dose dependency of cerebral blood flow. J Neurosci Methods 2009;179:22–8.

Phelps MT, Roberts WA. Central-place foraging by Rattus norvegicus on a radial maze. J Comp Psychol 1989;103:326–38.

Prieto E, Collantes M, Delgado M, Juri C, Garcia-Garcia L, Molinet F, et al. Statistical parametric maps of 18F-FDG PET and 3-D autoradiography in the rat brain: a cross-validation study. Eur J Nucl Med Mol Imaging 2011;38:2228–37.

Pyke GH. Optimal foraging theory – a critical review. Annu Rev Ecol Syst 1984;15:523–75.

Pyke GH, Pulliam HR, Charnov EL. Optimal foraging – selective review of theory and tests. Q Rev Biol 1977;52:137–54.

Qi J, Leahy RM, Cherry SR, Chatziioannou A, Farquhar TH. High-resolution 3D Bayesian image reconstruction using the microPET small-animal scanner. Phys Med Biol 1998;43:1001–13.

Raichle ME, Mintun MA. Brain work and brain imaging. Ann Rev Neurosci 2006;29:449–76.

Regenhardt RW, Ansari S, Azari H, Caldwell KJ, Mecca AP. Utilizing a cranial window to visualize the middle cerebral artery during endothelin-1 induced middle cerebral artery occlusion. J Vis Exp 2013;72:e50015.

Rempel-Clower NL. Role of orbitofrontal cortex connections in emotion. Ann N Y Acad Sci 2007;1121:72–86.

Rodgers RJ, Johnson NJ. Factor analysis of spatiotemporal and ethological measures in the murine elevated plus-maze test of anxiety. Pharmacol Biochem Behav 1995;52:297–303.

Roome RB, Bartlett RF, Jeffers M, Xiong J, Corbett D, Vanderluit JL. A reproducible endothelin-1 model of forelimb motor cortex stroke in the mouse. J Neurosci Methods 2014;233:34–44.

Rubin G, Levy EI, Scarrow AM, Firlik AD, Karakus A, Wechsler L, et al. Remote effects of acute ischemic stroke: a xenon CT cerebral blood flow study. Cerebrovasc Dis 2000;10:221–8.

Sakurada O, Kennedy C, Jehle J, Brown JD, Carbin GL, Sokoloff L. Measurement of local cerebral blood flow with iodo[14C]antipyrine. Am J Physiol 1978;234:H59–66.

Shih WJ, Huang WS, Milan PP. F-18 FDG PET demonstrates crossed cerebellar diaschisis 20 years after stroke. Clin Nucl Med 2006;31:259–61.

Sotres-Bayon F, Quirk GJ. Prefrontal control of fear: more than just extinction. Curr Opin Neurobiol 2010;20:231–5.

Soylu H, Zhang D, Buist R, Martin M, Albensi BC, Parkinson FE. Intracortical injection of endothelin-1 induces cortical infarcts in mice: effect of neuronal expression of an adenosine transporter. Exp Transl Stroke Med 2012;4:4.

Takahashi LK, Lore RK. Foraging and food hoarding of wild *Rattus norvegicus* in an urban environment. Behav Neural Biol 1980;29:527–31.

Takatsuru Y, Fukumoto D, Yoshitomo M, Nemoto T, Tsukada H, Nabekura J. Neuronal circuit remodeling in the contralateral cortical hemisphere during functional recovery from cerebral infarction. J Neurosci 2009;29:10081–6.

Tigner JC, Wallace RJ. Hoarding of food and non-food items in blind, anosmic and intact albino rats. Physiol Behav 1972;8:943–8.

Virley D, Hadingham SJ, Roberts JC, Farnfield B, Elliott H, Whelan G, et al. A new primate model of focal stroke: endothelin-1-induced middle cerebral artery occlusion and reperfusion in the common marmoset. J Cereb Blood Flow Metab 2004;24:24–41.

Vollmar S, Hampl JA, Kracht L, Herholz K. Integration of functional data (PET) into brain surgery planning and neuronavigation. Adv Med Eng 2007;114: 98–103.

Walberer M, Backes H, Rueger MA, Neumaier B, Endepols H, Hoehn M, et al. Potential of early [18F]-2-fluoro-2-deoxy-D-glucose positron emission tomography for identifying hypoperfusion and predicting fate of tissue in a rat embolic stroke model. Stroke 2012;43:193–8.

Ward NM, Sharkey J, Marston HM, Brown VJ. Simple and choice reaction-time performance following occlusion of the anterior cerebral arteries in the rat. Exp Brain Res 1998;123:269–81.

Welsh JP, Yuen G, Placantonakis DG, Vu TQ, Haiss F, O'Hearn E, et al. Why do Purkinje cells die so easily after global brain ischemia? Aldolase C, EAAT4, and the cerebellar contribution to posthypoxic myoclonus. Adv Neurol 2002;89:331–59.

Whishaw IQ. Time estimates contribute to food handling decisions by rats – implications for neural control of hoarding. Psychobiology 1990;18:460–6.

Whishaw IQ, Dringenberg HC. How does the rat (*Rattus norvegicus*) adjust food-carrying responses to the influences of distance, effort, predatory odor, food size, and food availability? Psychobiology 1991;19:251–61.

Whishaw IQ, Kornelsen RA. Two types of motivation revealed by ibotenic acid nucleus accumbens lesions: dissociation of food carrying and hoarding and the role of primary and incentive motivation. Behav Brain Res 1993;55:283–95.

Whishaw IQ, Tomie JA. Food-pellet size modifies the hoarding behavior of foraging rats. Psychobiology 1989;17:93–101.

Whishaw IQ, Tomie J. Piloting and dead reckoning dissociated by fimbria-fornix lesions in a rat food carrying task. Behav Brain Res 1997;89:87–97.

Whishaw IQ, Oddie SD, McNamara RK, Harris TL, Perry BS. Psychophysical methods for study of sensory-motor behavior using a food-carrying (hoarding) task in rodents. J Neurosci Methods 1990;32:123–33.

Whitman MC, Greer CA. Adult neurogenesis and the olfactory system. Prog Neurobiol 2009;89:162–75.

Wolfe JB. An exploratory study of food-storing in rats. J Comp Psychol 1939;28: 97–108.

Yorgason JT, Espana RA, Konstantopoulos JK, Weiner JL, Jones SR. Enduring increases in anxiety-like behavior and rapid nucleus accumbens dopamine signaling in socially isolated rats. Eur J Neurosci 2013;37:1022–31.